Journal of Operation and Automation in Power Engineering

Vol. 12, No. 1, Jan. 2024, Pages: 1-13

http://joape.uma.ac.ir

A MILP Model Incorporated With the Risk Management Tool for Self-Healing Oriented Service Restoration

N. Afsari, S. J. Seyedshenava, H. Shayeghi*

Department of Technical Engineering, University of Mohaghegh Ardabili, Ardabil, Iran

Abstract— *The inevitable emergence of intelligent distribution networks has introduced new features in these networks. According to most experts, self-healing is one of the main abilities of smart distribution networks. This feature increases the reliability and resiliency of networks by reacting fast and restoring the critical loads (CLs) during a fault. Nevertheless, the stochastic nature of the components in a power system imposes significant computational risk in enabling the system to self-heal. In this paper, a mathematical model is introduced for the self-healing operation of networked Microgrids (MGs) to assess the risk in the optimal service restoration (SR) problem. Electric vehicles (EVs) and plug-in hybrid electric vehicles (PHEVs) and their stochastic nature besides the distributed generation units (DGs), the ability to reconfiguration, and demand response program are considered simultaneously. The objective function is designed to maximize the restored loads and minimize the risk. The Conditional Value-at-Risk (CVaR) is used to calculate the risk of the SR as one of the most efficient and famous risk indices. In the general case study and considering β equal to the 0, 1, 2, 3, and 4, expected values of SR for the risk-averse problem is 21.2, 20, 19.3, 19.1, and 19% less than the risk-neutral problem, respectively. The formulation of the problem is mixed-integer linear programming (MILP), and the model is tested in the modified Civanlar test system. The analysis of several case studies has proved the performance of the proposed model and the importance of risk management in the problem.*

Keywords—Self-healing, Service restoration, Risk management, Microgrid, Distributed generation.

NOMENCLATURE

Indices and Sets

ω, Ω	Index and set of the scenarios [1:N$_\omega$]
b, B	Index and set of the electric vehicles' brand [1:N$_b$]
k, K	Index and set of the intervals in piecewise linearization [1:N$_k$]
n, N	Index and set of the network nodes [1:N$_n$]
SN	State Number of the network topology [1:N$_{SN}$]
t, T	Index and set of the timeslots [1:N$_t$]

Constants and parameters

α	Confidence level
β	Risk weight
$\chi^{n,b}$	The number of the EV b, in the node n
η^b_{CH} , η^b_{DCH}	Charging and discharging of the EV b
$\lambda^{t,\omega}_E$	Demand values of the load type E at time t
$\lambda^{t,\omega}_G$	Demand values of the load type G at time t
$\lambda^{t,\omega}_Q$	Demand values of the load type Q at time t
ϕ_ω	Occurrence probability of scenario ω
a_g , b_g , c_g	Coefficients of the function of the EGs power generation
$CVaR_\alpha$	CVaR with confidence level α
E^n	The size of the load type E in the node n
$g^{\max/\min}_{eg}$	Maximum/minimum limits of fuel consumption
G^n	The size of the load type G in the node n
$P^{t,\omega}_{DG1}$	Generation amount of DG1 at time t and scenario ω
$P^{t,\omega}_{DG2}$	Generation amount of DG2 at time t and scenario ω
$P^{t,\omega}_{DG3}$	Generation amount of DG3 at time t and scenario ω
P^t_s	Probability of clearing the fault at time t
Q^n	The size of the load type Q in the node n
$SOC^{\mathrm{b}}_{\max}$	Minimum SOC of the EV b
$SOC^{\mathrm{b}}_{\min}$	Maximum SOC of the EV b
$\mathrm{P}^{\mathrm{b}}_{\mathrm{CH-max}}$	maximum charging power of the EV b
$\mathrm{P}^{\mathrm{b}}_{\mathrm{DCH-max}}$	maximum discharging power of the EV b
Big M	Big number

Variables

$\Delta g^{b,k}_{eg}$	Length of block k of linearized fuel consumption of the EG b
η_ω, ζ	Auxiliary variables used in CVaR calculation
$\tau^{b,n,t,\omega}_{ch}$	binary variable, which indicates the operating charging status of the EV b in the node n, at time t, and scenario ω
$\tau^{b,n,t,\omega}_{dch}$	binary variable, which indicates the operating discharging status of the EV b in the node n, at time t, and scenario ω
$g^{b,k}_{eg,ini/fin}$	Initial and final values of fuel consumption in block k of linearized output of the EG b
$gk^{\mathrm{b,k,n,t},\omega}_{eg}$	operating kth section of linearized fuel consumption function of the EG b, in the node n, at time t, and in scenario ω
$s^{b,k}_{eg}$	Slope of fuel consumption in block k of linearized output of the EG b
$SOC^{\mathrm{b,n,t},\omega}$	Operating SOC of the EV b, in the node n, at time t, and scenario ω
$U^{n,t,\omega}$	Statues indicator of the load type E where 1 means satisfied and 0 means shed.
$V^{n,t,\omega}$	Statues indicator of the load type Q where 1 means satisfied and 0 means shed.
$Y^{n,t,\omega}$	Statues indicator of the load type G where 1 means satisfied and 0 means shed.
$\mathrm{g}^{\mathrm{b,n,t},\omega}_{eg}$	operating total fuel consumption function of the EG b, in the node n, at time t, and in scenario ω

Received: 26 Feb. 2022
Revised: 04 Jul. 2022
Accepted: 26 Jul. 2022
*Corresponding author:
E-mail: seyedshenava@uma.ac.ir (S. J. Seyedshenava)
DOI: 10.22098/joape.2023.10412.1740
Research Paper

$P^{b,n,t,\omega}_{CH-total}$ Total charging power of the EV b, in the node n, at time t, and scenario ω

$P^{b,n,t,\omega}_{CH}$ Charging power of the EV b, in the node n, at time t, and scenario ω

$P^{b,n,t,\omega}_{DCH-total}$ Total discharging power of the EV b, in the node n, at time t, and scenario ω

$P^{b,n,t,\omega}_{DCH}$ Discharging power of the EV b, in the node n, at time t, and scenario ω

$P^{b,n,t,\omega}_{EG-total}$ Total EG output of the EV b, in the node n, at time t, and scenario ω

$P^{b,n,t,\omega}_{EG}$ EG output of the EV b, in the node n, at time t, and scenario ω

1. Introduction

1.1. Aim

One of the important characteristics of the smart grids is resiliently operating in the hardware or software failures to enhance the level of the reliability and security of supplying energy [1]. Such capabilities in a self-heal scheme lead to a safe and reliable power supply for the consumers [2].

In the normal operation, the main grid supplies the loads, and the goal is to minimize the cost of the operation. When a fault happens, the model switches to the self-healing mode. To support the on-emergency portion of the system, DGs, energy storage systems (ESSs), vehicle-to-grids (V2Gs), and grid-to-vehicles (G2Vs) capability in EVs, PHEVs with engine generators (EGs), as well as remote control switches (RCSs) provide network maneuverability and optimal restore of CLs using available energy sources [3]. In other words, MGs operate autonomously in parallel with the traditional electricity *macrogrid*.

Depending on the level of automation in the self-heal power system, the fault will isolate, and the out-of-service zones will re-energize automatically. After the appearance of a fault, an optimum restoration scheme maximizes the number of restored costumes while satisfying operational and system constraints [4]. Because of the stochastic nature of the components, such problems have a great deal with the uncertainty that imposes significant computational risk. To control the risk of the uncertain data, a risk management tool is incorporated into the optimization problem, and necessary changes are done in the objective function and constraints. To take into account the risk associated with the fluctuation of the problem, this paper presents a MILP model to solve the unscheduled SR problem incorporated with conditional value-at-risk (CVaR) in the model.

1.2. Literature review

Optimal energy management between DGs in the MGs under normal operating conditions has been considered by researchers [5, 6]. For critical situations, reliability, resiliency, and security are the most important features of the self-heal smart grids. Due to the novelty of the self-healing issue, there is no single standard and definition. According to the report from National Energy Technology Laboratory (NETL), self-healing is the first of seven characteristics of a modern grid [7].

In [8], a multi-criteria optimization model is introduced to achieve self-healing, where the solution is chosen after the evaluation of technical indices such as branch load limits, active power losses, voltage deviation limits, and reliability indices. Artificial neural networks [9] and expert systems [10] as knowledge-based approaches have been suggested to solve the restoration problem effectively. By coordination feasible power interchanges between the MGs, a hierarchical outage management plan for Multi-MGs is suggested in [11]. Management of the uncertain parameters in MG is done by different methods such as the Coupla-base method for energy management in MG [12]. In [13], evaluation of uncertainty in multiple MGs is done by Monte Carlo simulation. Taguchi's orthogonal array testing method

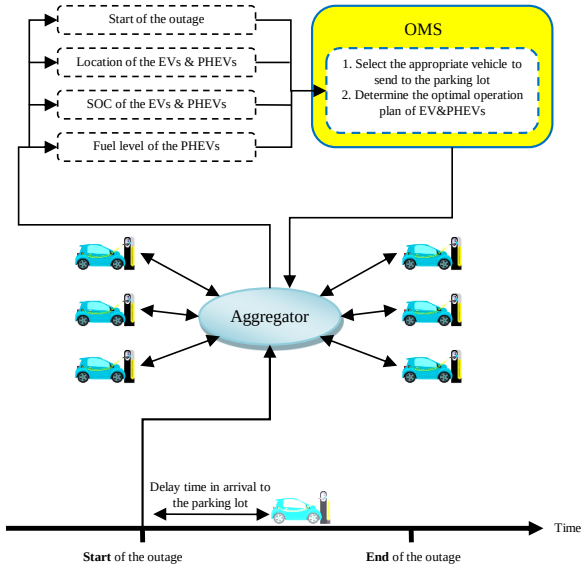

Fig. 1. The integration of an OMS network and EVs

in [14] is introduced according to robust design theory to select scenarios related to uncertain variables. A data-driven dynamic uncertainty bound estimation method is used in [15]. Chance constrained programming approach to handle the constraints under uncertainties is introduced in [16].

Risk management has already been used in some issues related to the power system. The energy market is one of the topics in which risk management is widely used [17–19]. In [20], a risk-assessment approach has been introduced to the evaluation of the reliability of a wind integrated power system for short-term operation planning. Besides reliability constraints in power systems, risk management tools are incorporated into the optimal expansion planning problem in [21]. In [22], RCS deployment in a distributed power system is introduced to evaluate the risk by a step-by-step method. An appropriate risk metric to assess the potential risk of sizing problem is incorporated in the optimal size of the hybrid power system component of the merchant marine vessel in [23].

1.3. Contribution

In the reviewed articles, although they have used risk management tool for assessment the power system problems, none of the self-healing field problems have discussed the risk management related to the SR problem. In this paper, a mathematical model for the SR problem is introduced by considering the risk management tool. The objective of this model is to maximize the expected restored loads and minimize the risk. The CVaR is used to account for the risk of the SR which has been widely used in risk management problems. The presence of an agent with a high probability and low profit needs to manage the risk of exposure to profit distribution with undesirable characteristics. In this condition, risk control is very important, and it should be imposed into the mathematical model of stochastic programming [24].

The most common way to manage the risk is to add a term to measure and control the risk of profit distribution in the formulation of the problem. Usually, this sentence is known as risk expression or risk measure. Some of the most relevant risk metrics regarding stochastic programming problems in the technical literature are [25]: (i) Variance, (ii) Shortfall probability, (iii) Expected shortage, (iv) Value-at-Risk (VaR), and (v) Conditional Value-at-Risk (CVaR).

Among the risk measures, the Conditional Value-at-Risk (CVaR) is the most advantageous for some reasons. In comparison to the first metric (Variance), we don't need to use any quadratic (or

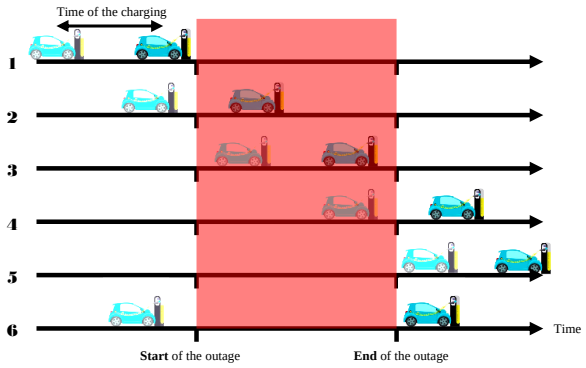

Fig. 2. Different scenarios based on the time of start and end of the outage and presence of an EV in the parking lot

nonlinear) term in this one. Therefore, it maintains linearity and we can use it in linear programming (LP) and mixed-integer LP (MILP) problems. Unlike the second and fourth cases, the CVaR does not change the dimensions of the problem by adding a binary variable. This maintains the convergence of the LP problem and does not add a variable to the MILP problem. Unlike all other measures, the CVaR can provide cost or profit information across the distribution search space, and because of the coherence of the CVaR, it satisfies all desirable characteristics for a risk metric. Additional information about these features is available in [24].

The problem is formulated as MILP, and the model is applied to the modified Civanlar (IEEE 13-buses) test system [26]. In several case studies, the impacts of risk weight, confidence level, and the presence of EVs & PHEVs as some important parameters are investigated to control the experiencing risk of SR problem. These analyses have verified the performance of the proposed model and proved the importance of the risk control issue when formulating stochastic programming models. In summary, this paper has prominent contributions as follows:

1) A mathematical model for SR including the sentences of CVaR and its constraints is introduced for the first time.
2) In this stochastic programming problem, the classification of load types is considered multi-stage, and the non-anticipativity of the decisions is established.
3) In both risk-neutral and risk-averse conditions, the expected SR versus the different risk management parameters is presented by the efficient frontier.
4) Unlike other studies, the ability to reconfiguration and demand response program in the presence of the electric vehicles and plug-in hybrid electric vehicles and their stochastic nature besides the distributed generation units are considered simultaneously.
5) According to the results, planning has been done dynamically instead of hour by hour and has led to more comprehensive results.

2. PROBLEM FORMULATION AND MODELING

2.1. Proposed risk-averse SR

The CVaR risk metric has the ability to incorporate into the minimization and maximization problems. These problems should define with discrete scenarios. Considering discrete scenarios in a maximization problem, the definition of CVaR can be explained as the expected value of the profit smaller than $(1-\alpha)$-quantile, where $\alpha\in(0,1)$ is the confidence level of scenarios. Since in the SR problem the objective is higher restored loads, the model maximizes the weighted sum of the SR with lower risk. CVaR by incorporation into the risk-neutral problem explains as follows [24]:

$$Maximize\ \ (1-\beta)\times profit+\beta\times CVaR_{\alpha} \tag{1}$$

$$profit=\sum_{\omega\in\Omega}\phi_{\omega}prof_{\omega},\ \ \forall\omega\in\Omega \tag{2}$$

Where, the CVaR for a discrete distribution is mathematically expressed as,

$$CVaR_{\alpha}=\zeta-\frac{1}{1-\alpha}\sum_{\omega\in\Omega}\phi_{\omega}\eta_{\omega},\ \ \forall\omega\in\Omega \tag{3}$$

$$\eta_{\omega}+\Pr of_{\omega}-\zeta\geq 0\ \ ,\ \ \forall\omega\in\Omega \tag{4}$$

$$\eta_{\omega}\geq 0\,,\ \ \forall\omega\in\Omega \tag{5}$$

Here, β is a non-negative weighting parameter and establishes a tradeoff between the risk and total of the restored loads; so that a higher value of β leads to more risk-averse for the system operator. In opposition, β = 0 implies a risk-neutral problem.

2.2. Objective function

In this SR problem, the objective function is formulated to find the optimal hourly operation of the MGs components including generators as distributed generation units and EVs, and PHEVs as energy storage systems by satisfying technical constraints. To minimize the unsupplied customers, SR problem incorporated with the risk management tool can determine the energizing schedule of the customers. The objective is the maximization of the expected supplied loads and finding the proper restorative zones in the network.

$$\begin{aligned}\underset{U^{n,t,\omega},V^{n,t,\omega},Y^{n,t,\omega},\xi,\eta_{\omega}}{Maximize}\ &\sum_{\omega\in\Omega}\phi_{\omega}\left\{\sum_{t\in T}Ps_{t}\left(\sum_{n\in N}\left(\lambda_{E}^{t,\omega}E^{n}U^{n,t,\omega}+\lambda_{Q}^{t,\omega}Q^{n}V^{n,t,\omega}+\lambda_{G}^{t,\omega}G^{n}Y^{n,t,\omega}\right)\right)\right\}\\&+\beta\left(\zeta-\frac{1}{1-\alpha}\sum_{\omega\in\Omega}\phi_{\omega}\eta_{\omega}\right);\quad\forall n\in N,\forall t\in T,\forall\omega\in\Omega\end{aligned} \tag{6}$$

Here, the first part of the objective function determines the total weighted loads during the periods of restoration. The second part deals with the risk management of the objective function. The power balance within each MG is expressed as:

$$\begin{aligned}&\sum_{N\in MG1}\left(E^{n}U^{n,t,\omega}+Q^{n}V^{n,t,\omega}+G^{n}Y^{n,t,\omega}\right)\leq\\&P_{DG1}^{t,\omega}+\sum_{N\in MG1}\left(P_{dch\_total}^{n,t,\omega}-P_{ch\_total}^{n,t,\omega}+P_{EG\_total}^{n,t,\omega}\right);\\&\forall n\in N,\forall t\in T,\forall\omega\in\Omega\end{aligned} \tag{7}$$

$$\begin{aligned}&\sum_{N\in MG2}\left(E^{n}U^{n,t,\omega}+Q^{n}V^{n,t,\omega}+G^{n}Y^{n,t,\omega}\right)\leq\\&P_{DG2}^{t,\omega}+\sum_{N\in MG2}\left(P_{dch\_total}^{n,t,\omega}-P_{ch\_total}^{n,t,\omega}+P_{EG\_total}^{n,t,\omega}\right);\\&\forall n\in N,\forall t\in T,\forall\omega\in\Omega\end{aligned} \tag{8}$$

$$\sum_{N\in MG3}\left(E^{n}U^{n,t,\omega}+Q^{n}V^{n,t,\omega}+G^{n}Y^{n,t,\omega}\right)\leq P_{DG3}^{t,\omega}+\sum_{N\in MG3}\left(P_{dch\_total}^{n,t,\omega}-P_{ch\_total}^{n,t,\omega}+P_{EG\_total}^{n,t,\omega}\right);\quad \forall n\in N,\forall t\in T,\forall\omega\in\Omega \tag{9}$$

2.3. Charge/discharge scheduling of the electric vehicles and plug-in hybrid electric vehicles

Extensive installation without major technical problems of EVs and PHEVs has made them the target of many studies. On the other hand, the integration of the PHEVs into the power systems is divided into two categories, known as the centralized and distributed charging modes. The first mode is used in large-scale parking lots or commercial charging stations, and the second is used by the owner of charging panels in residential complexes [27]. In general, the presence of an electric vehicle in the power system is considered as "noise" for the operator, so it is necessary to collect the information of electric vehicles in a large control center to create the necessary coordination between these vehicles and the power system [28]. The aggregators also have the task of discharge/charge scheduling of the PHEVs. In occurring a fault, electric vehicles that are not present in the parking lot can be managed by the Outage Management System (OMS). The data exchange between OMS and EV is shown in Fig. 1.

Considering that separating from the main grid is defined as a critical condition and the objective is the maximization of the SR, the storage energy systems will be in discharge mode. In this paper, six scenarios are considered for the fault conditions as Fig. 2. The classification of these scenarios is based on the presence of the vehicle in the parking lot at the time of the event when the MGs are separated from the main grid [29].

To analysis the EV & PHEVs behavior in SR problem, in the first step, the probabilistic model of available energy associated with EV & PHEVs in a parking lot in normal condition is formulated. Charging/discharging scheduling of a V2G and G2V capable EV can be modeled as:

$$0\leq P_{ch}^{\mathrm{b,n,t,\omega}}\leq P_{CH-\max}^{b}\times\tau_{ch}^{\mathrm{b,n,t,\omega}},\quad \forall b\in B,\forall n\in N,\forall t\in T,\forall\omega\in\Omega \tag{10}$$

$$0\leq P_{dch}^{\mathrm{b,n,t,\omega}}\leq P_{DCH-\max}^{b}\times\tau_{dch}^{\mathrm{b,n,t,\omega}},\quad \forall b\in B,\forall n\in N,\forall t\in T,\forall\omega\in\Omega \tag{11}$$

$$SOC_{\min}^{b}\leq SOC^{b,n,t,\omega}\leq SOC_{\max}^{b},\quad \forall b\in B,\forall n\in N,\forall t\in T,\forall\omega\in\Omega \tag{12}$$

$$SOC^{b,n,t+1,\omega}=SOC^{b,n,t,\omega}+\left(\tau_{ch}^{b,n,t,\omega}\times P_{ch}^{b,n,t,\omega}\times\eta_{ch}^{b}-\frac{\tau_{dch}^{b,n,t,\omega}\times P_{dch}^{b,n,t,\omega}}{\eta_{dch}^{b}}\right)\Delta t,\quad \forall b\in B,\forall n\in N,\forall t\in T,\forall\omega\in\Omega \tag{13}$$

$$\tau_{ch}^{b,n,t,\omega}+\tau_{dch}^{b,n,t,\omega}\leq 1\ \forall b\in B,\forall n\in N,\forall t\in T,\forall\omega\in\Omega \tag{14}$$

$$SOC_{arr}^{b,n,t,\omega}=SOC_{initial}^{b,n,t,\omega}\ \forall b\in B,\forall n\in N,\forall t\in T,\forall\omega\in\Omega \tag{15}$$

$$SOC_{dep}^{b,n,t,\omega}=SOC_{final}^{b,n,t,\omega}\ \forall b\in B,\forall n\in N,\forall t\in T,\forall\omega\in\Omega \tag{16}$$

Control variables are applied in the charge and discharge limit of the EV & PHEVs according to constraints (10) and (11), respectively. Constraint (12) prevents the SOC from exceeding the allowable min and max levels. The SOC of each storage system is calculated in constraint (13). Constraint (14) ensures that simultaneous charging and discharging modes do not occur on storage systems per hour. Constraints (15) and (16) are used to force the SOC of the EV & PHEVs at the arriving time and departure time to be equal to the initial and final expected SOC, respectively.

The total charge and discharge power of energy storage systems are determined based on the number of different brands of electric vehicles, the amount of charge or discharge power of each brand, and also the status of the binary control variable of charge or discharge according to Eqs. (17–18).

$$P_{ch\_total}^{n,t,\omega}=\sum_{b\in B}\chi^{n,b}\times P_{ch}^{b,n,t,\omega}\times\tau_{ch}^{b,n,t,\omega};\quad \forall b\in B,\forall n\in N,\forall t\in T,\forall\omega\in\Omega \tag{17}$$

$$P_{dch\_total}^{n,t,\omega}=\sum_{b\in B}\chi^{n,b}\times P_{dch}^{b,n,t,\omega}\times\tau_{dch}^{b,n,t,\omega};\quad \forall b\in B,\forall n\in N,\forall t\in T,\forall\omega\in\Omega \tag{18}$$

This part of the problem is a nonlinear form by multiplying two continuous and binary variables. To solve the problem with the MILP method, it is necessary to linearize this part of the problem, which is done by the "big-M" method [30]. All big-M parameters in the model formulation are set to big enough, which is sufficiently higher than the charge and discharge power capacity of all EV & PHEVs.

$$P_{ch\_total}^{n,t,\omega}-\sum_{b\in B}\chi^{n,b}\times P_{ch}^{b,n,t,\omega}\leq\left(1-\tau_{ch}^{b,n,t,\omega}\right)\times bigM;\quad \forall b\in B,\forall n\in N,\forall t\in T,\forall\omega\in\Omega \tag{19}$$

$$P_{ch\_total}^{n,t,\omega}-\sum_{b\in B}\chi^{n,b}\times P_{ch}^{b,n,t,\omega}\geq-\left(1-\tau_{ch}^{b,n,t,\omega}\right)\times bigM;\quad \forall b\in B,\forall n\in N,\forall t\in T,\forall\omega\in\Omega \tag{20}$$

$$P_{ch}^{b,n,t,\omega}\leq P_{ch\_\max}^{b,n,t,\omega}\times\tau_{ch}^{b,n,t,\omega};\quad \forall b\in B,\forall n\in N,\forall t\in T,\forall\omega\in\Omega \tag{21}$$

$$P_{dch\_total}^{n,t,\omega}-\sum_{b\in B}\chi^{n,b}\times P_{dch}^{b,n,t,\omega}\leq\left(1-\tau_{dch}^{b,n,t,\omega}\right)\times bigM;\quad \forall b\in B,\forall n\in N,\forall t\in T,\forall\omega\in\Omega \tag{22}$$

$$P_{dch\_total}^{n,t,\omega}-\sum_{b\in B}\chi^{n,b}\times P_{dch}^{b,n,t,\omega}\geq-\left(1-\tau_{dch}^{b,n,t,\omega}\right)\times bigM;\quad \forall b\in B,\forall n\in N,\forall t\in T,\forall\omega\in\Omega \tag{23}$$

$$P_{dch}^{b,n,t,\omega}\leq P_{dch\_\max}^{b,n,t,\omega}\times\tau_{dch}^{b,n,t,\omega};\quad \forall b\in B,\forall n\in N,\forall t\in T,\forall\omega\in\Omega \tag{24}$$

Table 1. Scenarios related to the value of the load demands

Load	Type E				Type Q				Type G			
	Period				Period				Period			
Scenario	1	2	3	4	1	2	3	4	1	2	3	4
1	11	16.5	12.1	10	5.5	8.5	6.5	5	17	28	15	12
2	11	16.5	12.1	10	5.5	8.5	6.5	5	10	17	13	13
3	11	16.5	12.1	10	5	7	5.5	6	12	17	15	14
4	11	16.5	12.1	10	5	7	5.5	6	9	14	11	15
5	13.2	18.7	16.5	12	6.5	9.5	8	7	17	22	19	14
6	13.2	18.7	16.5	12	6.5	9.5	8	7	14	19	15	13
7	13.2	18.7	16.5	12	6	8.5	7.5	5	16	25	21	12
8	13.2	18.7	16.5	12	6	8.5	7.5	5	13	17	14	11
9	15.4	19.8	17.6	14	7	10.5	10.5	4	17	28	24	12
10	15.4	19.8	17.6	14	7	10.5	10.5	4	14	23	20	13
11	15.4	19.8	17.6	14	6.5	9	9.5	7	16	23	21	14
12	15.4	19.8	17.6	14	6.5	9	9.5	7	13	19	18	15

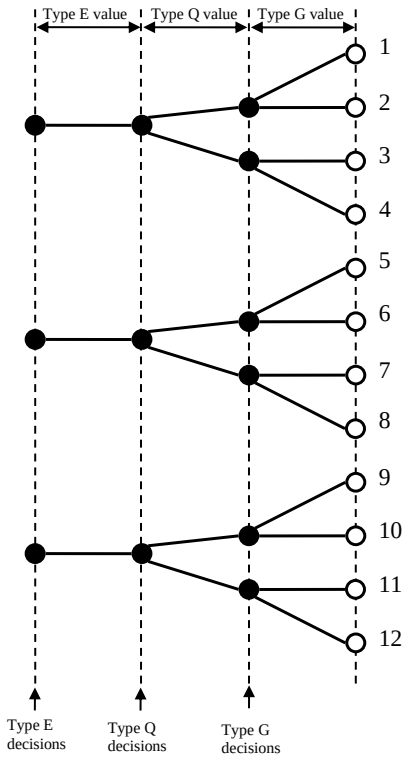

Fig. 3. Three-stage scenario tree of the load demand values: Type E, Type Q, Type G

Table 2. Load sizes of each bus (kW) [34]

Bus	E	Q	G
1	100	60	30
2	45	30	15
3	30	20	10
4	25	15	5
5	70	40	20
6	60	50	25
7	20	10	5
8	30	20	10
9	25	20	10
10	95	60	30
11	30	20	30
12	40	25	15
13	35	20	10

2.4. Modeling and operation constraints of the engine generators embedded in PHEVs

Due to the increased need for power in PHEV on trips above 350 miles, an EG is installed on PHEV [29]. The bulky EG fuel tank can assist in emergency load restoration. EG modeling is based on the conversion of the chemical energy of fuel into electrical energy. The ratio of fuel consumption to power production is referred to as brake-specific fuel consumption (BSFC), which is (g/kWh). The generating power of the generator at an operating point is determined for a certain speed and torque. The amount of fuel consumed at an operating point can be calculated using parameter BSFC. This amount will be equal to the fuel consumed in the EG per minute. Using measured data and estimated curve, a quadratic sample equation is obtained for an EG [31]. For example, the output power and fuel consumption of the "Chevrolet Volt" have a relation according to Eq. (25) [29]. In this equation, g(t) is the fuel consumed per hour t and P(g(t)) is the power produced by EG per hour. The time step considered in this equation is hourly.

$$P(g(t)) = -0.000105 \times g(t)^2 + 5.291 \times g(t) + 588.3\,;\ \forall t \in T \quad (25)$$

Due to the non-linear relationship between fuel consumption and EG power production, in this section, it is necessary to approximate with the linear piecewise function. Thus the nonlinear relation for each EG is converted to linear constraints Eqs. (26–34).

$$0 \le gk_{eg}^{\mathrm{b,k,n,t,\omega}} \le \Delta g_{eg}^{b,k} \quad \forall b \in B, \forall k \in K, \forall n \in N, \forall t \in T, \forall \omega \in \Omega \quad (26)$$

$$\Delta g_{eg}^{b,k} = \frac{g_{eg}^{\max} - g_{eg}^{\min}}{K}\ ;\ \ \forall b \in B, \forall k \in K \quad (27)$$

$$g_{eg,ini}^{b,k} = (k-1)\Delta g_{eg}^{b,k} + g_{eg}^{\min}\ ;\ \ \forall b \in B, \forall k \in K \quad (28)$$

$$g_{eg,fin}^{b,k} = \Delta g_{eg}^{b,k} + g_{eg,ini}^{b,k}\,;\ \forall b \in B, \forall k \in K \quad (29)$$

$$g_{eg}^{b,n,t,\omega} = g_{eg}^{\min} + \sum_{k \in K} g_{eg}^{b,k,n,t,\omega}; \quad \forall b \in B, \forall k \in K, \forall n \in N, \forall t \in T, \forall \omega \in \Omega \quad (30)$$

$$s_{eg}^{b,k} = \frac{P_{eg,fin}^{b,k} - P_{eg,ini}^{b,k}}{\Delta g_{eg}^{b,k}}\,;\ \forall b \in B, \forall k \in K \quad (31)$$

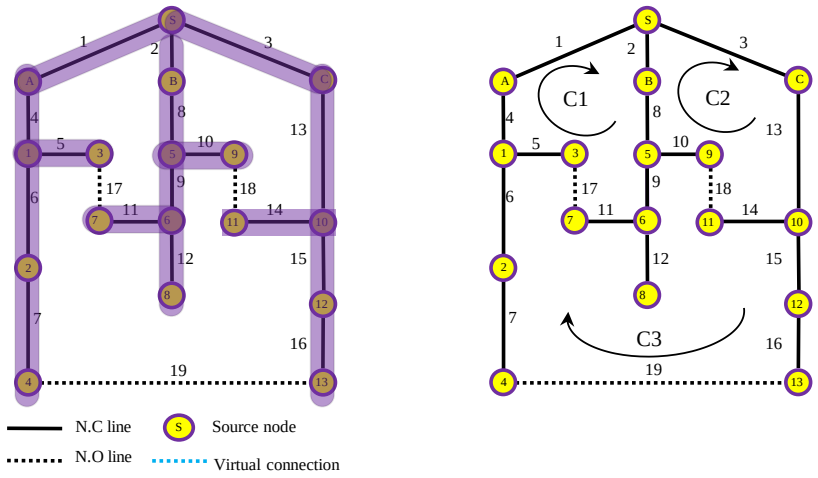

(a)

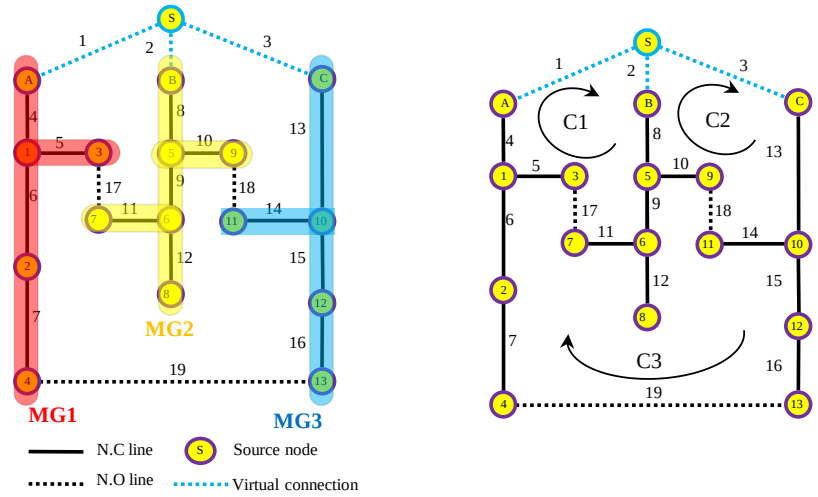

(b)

Fig. 4. Branch-node (Graph) model of network in (a) normal operation, (b) self-healing operation

$$P_{eg,ini}^{b,k} = -0.00105 \times (g_{eg,ini}^{b,k})^2 + 5.291 \times g_{eg,ini}^{b,k} + 588.3\,; \quad \forall b \in B, \forall k \in K \quad (32)$$

$$P_{eg,fin}^{b,k} = -0.00105 \times (g_{eg,fin}^{b,k})^2 + 5.291 \times g_{eg,fin}^{b,k} + 588.3\,; \quad \forall b \in B, \forall k \in K \quad (33)$$

$$P_{eg}^{b,n,t,\omega} = a_g \times (g_{eg}^{\min})^2 + b_g \times g_{eg}^{\min} + c_g + \sum_{K} s_{eg}^{b,k} \times g_{eg}^{b,k,n,t,\omega}; \quad \forall b \in B, \forall k \in K, \forall n \in N, \forall t \in T, \forall \omega \in \Omega \quad (34)$$

Finally, the total output power of EGs by different brands in each bus is calculated as follows.

$$P_{EG\_total}^{n,t,\omega} = \sum_{b \in B} \chi^{n,b} \times P_{eg}^{b,n,t,\omega}; \quad \forall b \in B, \forall n \in N, \forall t \in T, \forall \omega \in \Omega \quad (35)$$

2.5. Uncertainty modeling based on non-anticipativity

In this paper, the decision-making problem comprises several stages without perfect information. In this way, we go to the multi-stage stochastic programming method [32]. In all multi-stage stochastic programming problems, it is necessary to use the non-anticipativity concept in the decisions. That is, the values of the decision variables must be identical up to stage k if the realizations of the stochastic processes are identical up to stage k [26].

For this problem, the architecture of the scenario tree of the load demand values has exhibited in Fig 3, according to the data in Table 1. The number of scenarios is equal to 12 and the probability of occurrence of scenarios is considered equal. In this case, scenarios 1–4, 5–8, and 9–12 have the same type E values, while type Q values for scenarios 1–2, 3–4, and etc. are similar. Type G values are different for all scenarios.

To establish the non-anticipativity of the decisions, the values of the vectors A^E, A^Q, and A^G are Set up according to the structure of the tree for type E, type Q, and type G load values, respectively. Vectors A^E and A^Q for the tree in Fig 3 are:

$$A^E = A^Q = [1, 1, 1, 0, 1, 1, 1, 0, 1, 1, 1, 0] \quad (36)$$

The vector of A^G is defined as

$$A^G = [1, 0, 1, 0, 1, 0, 1, 0, 1, 0, 1, 0] \quad (37)$$

According to Table 1 and Fig 3, the matrix O^E used to sort the load values of type E for each period t in an increasing procedure for every scenario ω and to enforce non-decreasing value curves expressed as

$$O^E = \begin{bmatrix} 1 & 1 & 1 & 1 & 2 & 2 & 2 & 2 & 3 & 3 & 3 & 3 \\ 1 & 1 & 1 & 1 & 2 & 2 & 2 & 2 & 3 & 3 & 3 & 3 \\ 1 & 1 & 1 & 1 & 2 & 2 & 2 & 2 & 3 & 3 & 3 & 3 \\ 1 & 1 & 1 & 1 & 2 & 2 & 2 & 2 & 3 & 3 & 3 & 3 \end{bmatrix} \quad (38)$$

To enforce the non-decreasing value of the load demands curves, the non-anticipativity constraints are formulated as below,

$$U^{n,t,\omega} - U^{n,t,\omega'} \leq 0 \, \forall n \in N, \forall t \in T, \forall \omega \in \Omega \; ; \\ O^E(t,\omega) + 1 = O^E(t,\omega'), \; if \; A^E(\omega) = A^E(\omega') = 0 \quad (39)$$

$$U^{n,t,\omega} - U^{n,t,\omega+1} = 0 \, , \\ \forall n \in N, \forall t \in T, \forall \omega \in \Omega \, if \; A^E(\omega) = 1 \quad (40)$$

$$V^{n,t,\omega} - V^{n,t,\omega+1} = 0 \, , \\ \forall n \in N, \forall t \in T, \forall \omega \in \Omega \; ; \quad if \; A^Q(\omega) = 1 \quad (41)$$

$$Y^{n,t,\omega} - Y^{n,t,\omega+1} = 0 \, , \\ \forall n \in N, \forall t \in T, \forall \omega \in \Omega \; ; \quad if \; A^G(\omega) = 1 \quad (42)$$

2.6. General connectivity constraints

Another constraint that must be observed in the reconfiguration of the network is the maintenance of the radiality limitation of the network at the same time as the connection of all buses to the slack bus. On the other hand, one of the characteristics of a self-healing system is fast load restoration. Therefore, the fast execution of the program is very important in these studies.
Considering this reason, in this paper, the fundamental loops according to graph theory are used for the restoration of MGs. Based on this theory, an equivalent graph model is formed for each network, including nodes (buses) and branches (lines). It is assumed that all of the distributed generation recourses can control the frequency. So, with the occurrence of fault and disconnection from the upstream network, three MGs are formed according to Fig **??**, and distributed generation sources in A, B, and C play the role of the slack bus in power supply. Then fundamental loops are formed according to graph theory. Considering Fig **??**, the studied system has three fundamental loops (C1–C3). It should be noted that the number of fundamental loops (FL) is obtained by subtracting the number of branches from the nodes plus one (nb-nt+1). Each loop also contains a set of controllable switches. Further details are available in [33]. According to Fig **??**, the fundamental loop vectors (FLVs) will be as follows:

$$FLV_1 = \{L_1, L_2, L_4, L_5, L_8, L_9, L_{11}, L_{17}\} \quad (43)$$

$$FLV_2 = \{L_2, L_3, L_8, L_{10}, L_{13}, L_{14}, L_{18}\} \quad (44)$$

$$FLV_3 = \{L_1, L_3, L_4, L_6, L_7, L_{13}, L_{15}, L_{16}, L_{19}\} \quad (45)$$

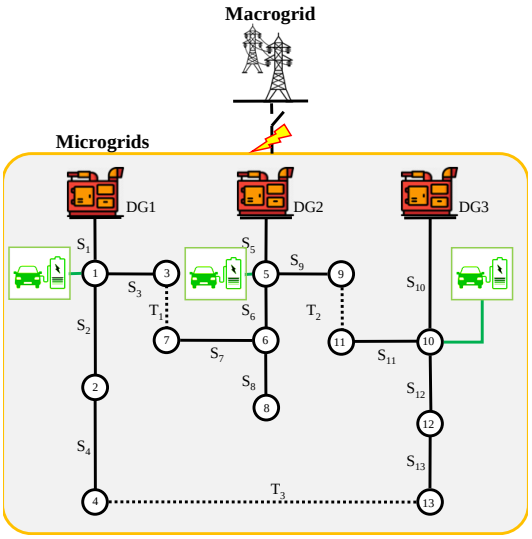

Fig. 5. Network configuration consisting of DGs & parking lots.

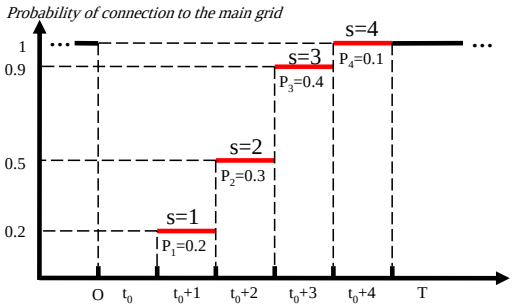

Fig. 6. Cumulative probability of the fault clearing

3. NUMERICAL RESULTS

In this section, the introduced model to solve the SR problem is validated using numerical results. First, the studied network is introduced. Then, the results of the SR problem in the self-healing mode, which is done in the risk management framework, are presented. In this section, the uncertainties related to the value of the loads are classified according to the topic of non-anticipativity. According to the scenario tree, the necessary constraints are defined and added to the problem. The efficiency of the proposed method in solving the SR problem in self-healing mode has been proved by presenting the results for different β coefficients. The mathematical model is formulated as a MILP problem, and the code for the model is written in GAMS 24.2.2 and solved by CPLEX solver. All the input data of the problem are entered in MATLAB R2013a and linked with GAMS through gdx.

3.1. Studied network

As mentioned earlier, the method of implementing the SR approach is applied to the modified Civanlar system in island mode. The system includes three DGs as distributed generation resources and electric vehicles as energy storage systems, according to Fig 5. The loads in each bus are divided into three types (E, Q, and G), and the load size s in kW are presented in Table 2. For simplicity, we ignore the changes in load over time, but the changes in the value of loads over time are already presented in Table 1.

The generation of DGs connected to basses 1, 5, and 10 in the time of outage is equal to (80, 80, 80, 80), (70, 75, 60, 70), and (50, 55, 65, 60) kW, respectively. The information of EVs and

Table 3. Operational details of the EVs & PHEVs [29]

ID of EV	EV type	Battery capacity (kWh)	Discharge power (kW)	EG maximum generation power (kW)	Gasoline tanker capacity (kg)
1	BEV	62	6.6	-	-
2	BEV	79.5	11.5	-	-
3	BEV	60	7.2	-	-
4	PHEV	40	6.6	45	13
5	PHEV	38.3	7.2	45	18
6	BEV	100	11	-	-
7	BEV	50	11	-	-
8	BEV	62	11.5	-	-

Table 4. Results of service restoration with various β in case 1

	β=0		β=1		β=2		β=3	
	SR	η_ω	SR	η_ω	SR	η_ω	SR	η_ω
ω1	3788.6	0	3572.6	0	2934.3	0	2774.8	0
ω2	2797.1	0	2833.1	0	2805.3	0	2755.8	0
ω3	3036.1	0	3000.1	0	2972.3	0	2812.8	0
ω4	2484.6	0	2556.5	276.5	2695.3	110	2755.8	0
ω5	3854	0	3717.3	0	3534.1	0	3396.6	0
ω6	3264.6	0	3235.8	0	3219.1	0	3301.6	0
ω7	4094.6	0	3993.8	0	3644.1	0	3396.6	0
ω8	3005.6	0	3012.8	0	3107.1	0	3244.6	0
ω9	4529.3	0	4529.3	0	4074.2	0	3722.2	0
ω10	3955.8	0	3955.8	0	3778.2	0	3646.2	0
ω11	4029.8	0	4029.8	0	3852.2	0	3665.2	0
ω12	3585.8	0	3585.8	0	3630.2	0	3608.2	0
Expected SR	3535.5		3501.9		3353.9		3256.7	
CVaR	2484.6		2602.6		2713.6		2755.5	
ζ	2484.6		2833.1		2805.3		2755.5	
Lines opened	17-18-19 (#1)		17-18-19 (#1)		17-18-19 (#1)		17-18-19 (#1)	
	17-18-19 (#2)		17-18-19 (#2)		17-18-19 (#2)		17-18-19 (#2)	
	17-18-19 (#3)		17-18-19 (#3)		17-18-19 (#3)		17-18-19 (#3)	
	17-18-19 (#4)		17-18-19 (#4)		17-18-19 (#4)		17-18-19 (#4)	

Table 5. Results of service restoration with various β in case 2

	β=0		β=1		β=2		β=3		β=4	
	SR	η_ω	SR	η_ω	SR	η_ω	SR	η_ω	SR	η_ω
ω1	11012	0	10822	0	10720	0	10652	0	10620	0
ω2	9930.3	0	9961.9	0	9945.6	0	9937.3	0	9936	0
ω3	10116	0	10085	0	10074	0	10043	0	10033	0
ω4	9505.6	0	9568.8	393.08	9621.3	324.27	9633.2	304.11	9638.2	297.73
ω5	12751	0	12654	0	12585	0	12558	0	12540	0
ω6	12098	0	12070	0	12064	0	12080	0	12077	0
ω7	13004	0	12942	0	12810	0	12761	0	12736	0
ω8	11770	0	11778	0	11814	0	11841	0	11841	0
ω9	14259	0	14259	0	14086	0	14017	0	13984	0
ω10	13594	0	13594	0	13527	0	13501	0	13482	0
ω11	13631	0	13631	0	13563	0	13527	0	13504	0
ω12	13117	0	13117	0	13134	0	13129	0	13118	0
Expected SR	12066		21675		31346		41025		50711	
CVaR	9505.6		9634.3		9675.4		9683.9		9687.9	
ζ	9505.6		9661.9		9945.6		9937.3		9936	
Lines opened	17-18-19 (#1)		17-18-19 (#1)		17-18-19 (#1)		17-18-19 (#1)		17-18-19 (#1)	
	17-18-19 (#2)		17-18-19 (#2)		17-18-19 (#2)		17-18-19 (#2)		17-18-19 (#2)	
	17-18-19 (#3)		17-18-19 (#3)		17-18-19 (#3)		17-18-19 (#3)		17-18-19 (#3)	
	17-18-19 (#4)		17-18-19 (#4)		17-18-19 (#4)		17-18-19 (#4)		17-18-19 (#4)	

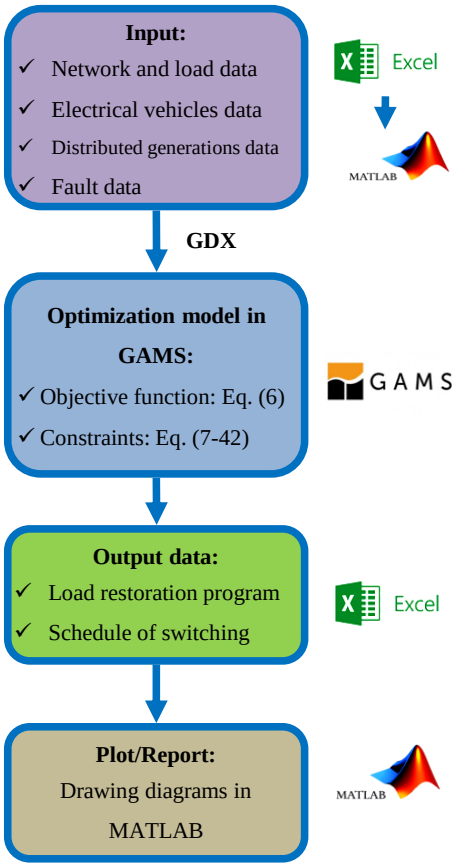

Fig. 7. The flowchart of the proposed method for self-healing oriented service restoration

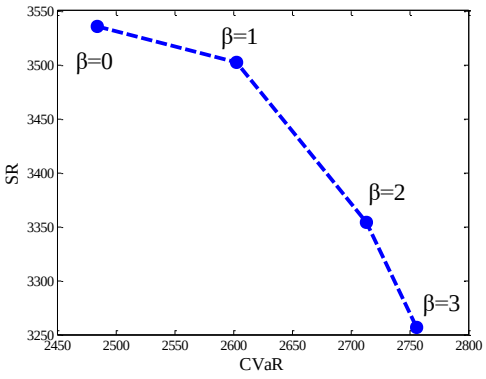

Fig. 8. SR versus CVaR (efficient frontier) in case 1

PHEVs is shown in Table 3. Location of parking lots is considered on buses 1, 5, and 10. The number of electric vehicles presented in the parking lot at the time of the event and the charge of battery and fuel level of these vehicles are considered random because of the random nature of these variables.

3.2. Case studies

The outage duration of the MGs from the upstream network is uncertain and considered to be 4 hours. Also, we consider the possibility of repairing and reconnecting the MGs to the macrogrid during these four hours, 0.2, 0.3, 0.4, and 0.1, and the cumulative probability of the fault clearing is shown in Fig 6.

Parking lots are connected to buses 1, 5, and 10, and the power exchange of these vehicles with the network is done through these

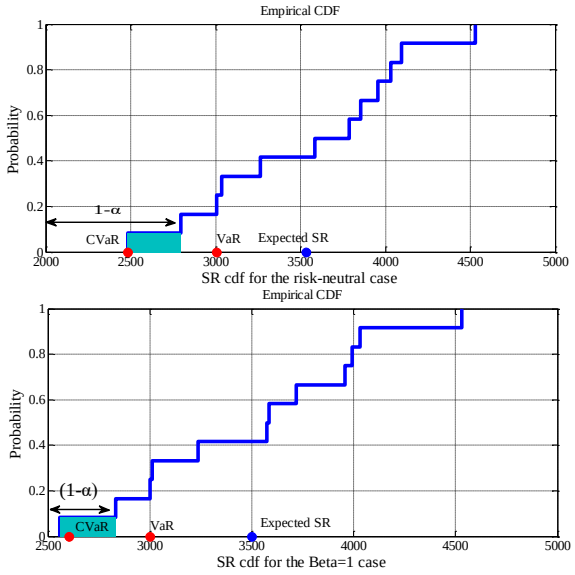

Fig. 9. Cdfs for $\beta = 0$ and $\beta = 1$

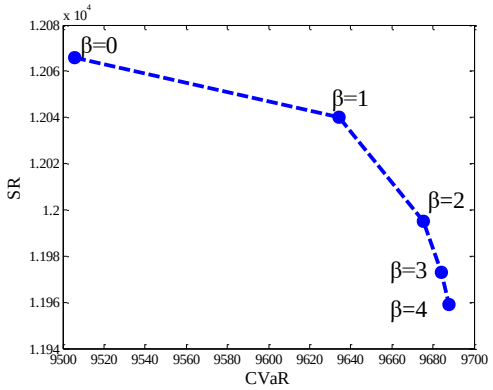

Fig. 10. SR versus CVaR (efficient frontier) in case 2

buses. In a general case, it is assumed that there are 3 electric vehicles for each type and totally 24 vehicles in the MGs. The number of electric vehicles in the parking lot at the time of the fault and the state of charge and fossil fuel level are also considered random. The program execution process is summarized in Fig 7.

A) Case study 1

In this case, the network is considered without the ability to switching and reconfiguration. Also, the effect of the presence of electric vehicles has been ignored. By disconnecting the upstream network, the distributed energy sources start to restore the loads for a 4-hour period until reconnection to the upstream grid. To analyze the impact of β, this parameter is gradually increased from 0 to 3, and the simulation is repeated. The confidence level is assumed to be α=0.9. The simulation results are presented in Table 4 and Fig 8. For β changes from 0 to 3, it is observed that the value of expected SR changes from 3535.5 to 3256.7 and the value of CVaR from 2484.6 to 2755.8.

It is observed that in *risk-averse* self-healing mode (β>0), the system prefers to restore the loads (expected SR) less than the *risk-neutral* (β=0) circumstance. Also, the optimal value of objective, i.e., optimal restored loads, has a trend for changes in a specific interval for beta, and these changes occur discretely.

Fig 9 represents the cumulative distribution functions for $\beta = \{0, 1\}$. For $\beta = 0$, the CVaR is equal to 2484.6, whereas it is equal to 2602.6 for $\beta = 1$. The worst scenario in each case has the highest robustness between the solutions. By comparing the results

Table 6. Results of service restoration with various β in case 3

	β=0		β=1		β=2		β=3	
	SR	η_ω	SR	η_ω	SR	η_ω	SR	η_ω
ω1	3848.7	0	3620.7	0	2947.9	0	2779.7	0
ω2	2803.2	0	2841.2	0	2811.9	0	2759.7	0
ω3	3055.2	0	3017.2	0	2987.9	0	2819.7	0
ω4	2473.7	0	2549.7	291.5	2695.9	0	2759.7	0
ω5	3883.5	0	3739.2	0	3546.1	116	3401.1	0
ω6	3262.1	0	3231.7	0	3214.1	0	3301.1	0
ω7	4137	0	4030.7	0	3662.1	0	3401.1	0
ω8	2989.1	0	2996.7	0	3096.1	0	3241.1	0
ω9	4579.5	0	4579.5	0	4099.8	0	3728.6	0
ω10	3975	0	3975	0	3787.8	0	3648.6	0
ω11	4053	0	4053	0	3865.8	0	3668.6	0
ω12	3585	0	3585	0	3631.8	0	3608.6	0
Expected SR	3553.7		3518.3		3362.3		3259.8	
CVaR	2473.7		2598.2		2715.2		2759.7	
ζ	2473.7		2841.2		2811.9		2759.7	
Lines opened	16-17-18 (#1)		17-18-19 (#1)		16-17-18 (#1)		5-18-19 (#1)	
	16-17-18 (#2)		16-17-18 (#2)		16-17-18 (#2)		16-17-18 (#2)	
	16-17-18 (#3)		16-17-18 (#3)		16-17-18 (#3)		17-18-19 (#3)	
	16-17-18 (#4)		16-17-18 (#4)		16-17-18 (#4)		16-17-18 (#4)	

Table 7. Results of service restoration with various β in case 4

	β=0		β=1		β=2		β=3		β=4	
	SR	η_ω	SR	η_ω	SR	η_ω	SR	η_ω	SR	η_ω
ω1	11012	0	10823	0	10721	0	10653	0	10621	0
ω2	9931.2	0	9962.8	0	9946.5	0	9938.2	0	9936.9	0
ω3	10118	0	10087	0	10076	0	10045	0	10035	0
ω4	9507.4	0	9570.6	392.19	9623.1	323.38	9635	303.22	9640	296.84
ω5	12758	0	12651	0	12581	0	12554	0	12536	0
ω6	12104	0	12077	0	12071	0	12087	0	12084	0
ω7	13012	0	12939	0	12807	0	12758	0	12732	0
ω8	11778	0	11785	0	11821	0	11848	0	11848	0
ω9	14280	0	14280	0	14108	0	14038	0	14005	0
ω10	13615	0	13615	0	13548	0	13522	0	13503	0
ω11	13643	0	13643	0	13576	0	13539	0	13517	0
ω12	13129	0	13129	0	13146	0	13142	0	13130	0
Expected SR	12074		12047		12002		11980		11966	
CVaR	9507.4		9636		9677		9685.5		9689.5	
ζ	9507.4		9962.8		9946.5		9938.2		9936.9	
Lines opened	17-18-19 (#1)		16-17-18 (#1)		5-18-19 (#1)		16-17-18 (#1)		16-17-18 (#1)	
	16-17-18 (#2)		16-17-18 (#2)		16-17-18 (#2)		16-17-18 (#2)		16-17-18 (#2)	
	17-18-19 (#3)		16-17-18 (#3)		17-18-19 (#3)		17-18-19 (#3)		16-17-18 (#3)	
	16-17-18 (#4)		16-17-18 (#4)		16-17-18 (#4)		16-17-18 (#4)		16-17-18 (#4)	

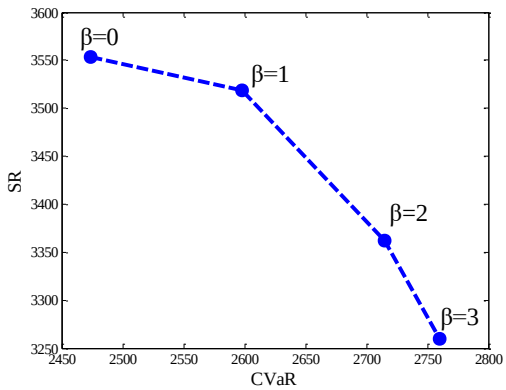

Fig. 11. SR versus CVaR (efficient frontier) in case 3

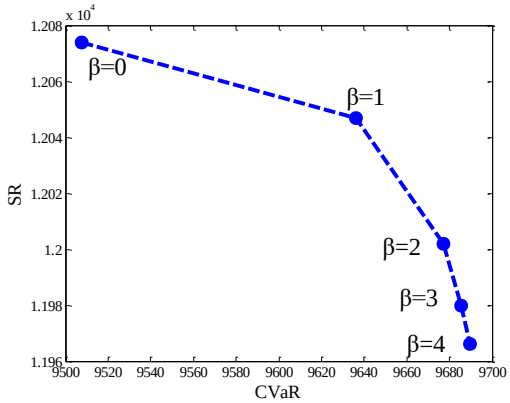

Fig. 12. SR versus CVaR (efficient frontier) in case 4

of the expected SR and CVaR (or VaR) for $\beta = \{0, 1, 2, 3\}$, it can be seen that by using the risk management tool, the robustness of the obtained solutions have been increased.

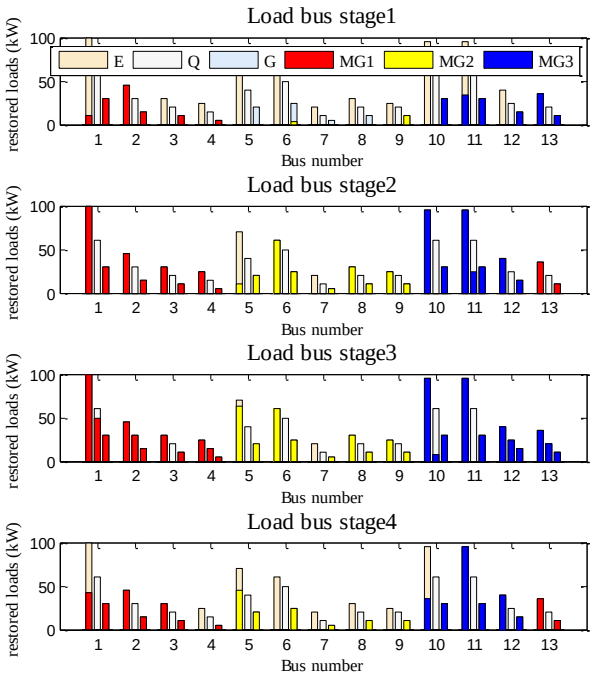

(a) β=0, ω=11

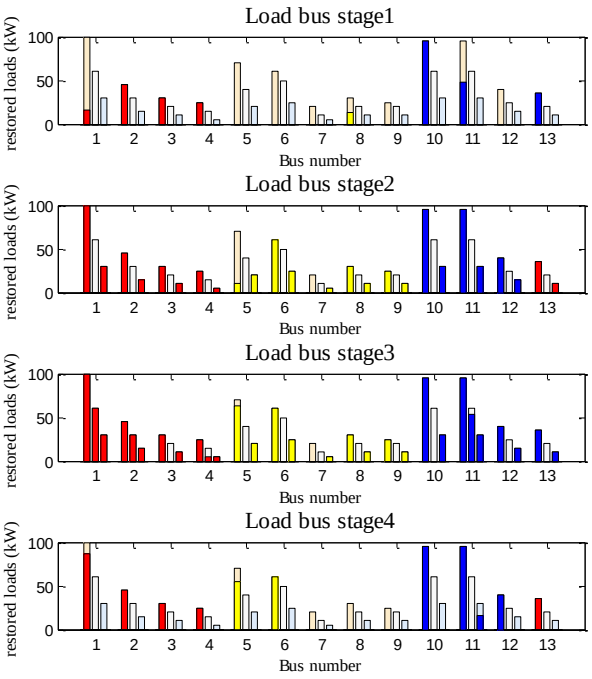

(b) β=0, ω=4

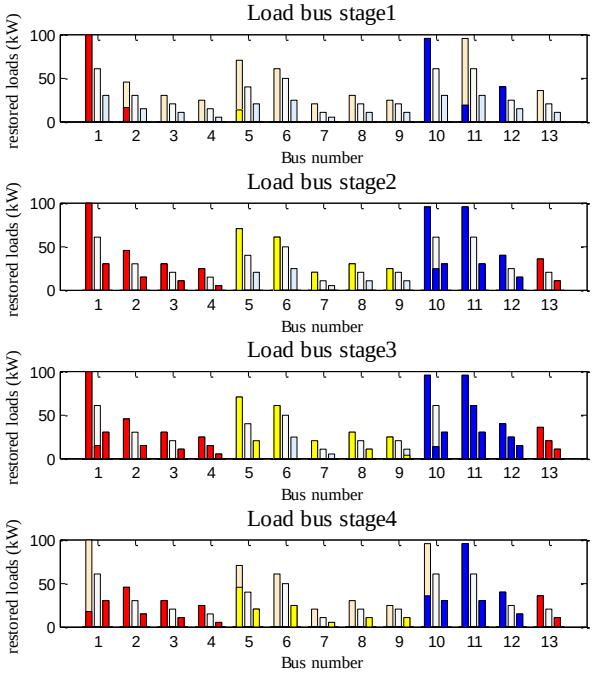

(c) β=4, ω=11

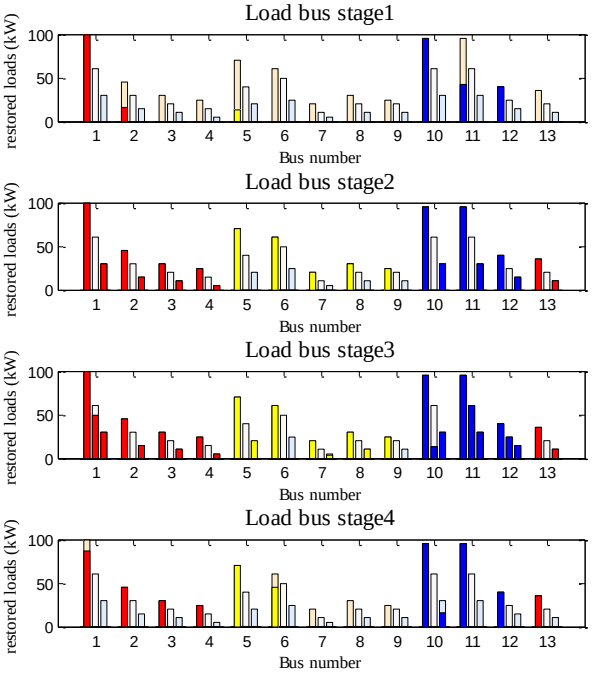

(d) β=4, ω=4

Fig. 13. schedule in four-time steps and different buses of (a)&(b) β=0, and (c)&(d) β=4.

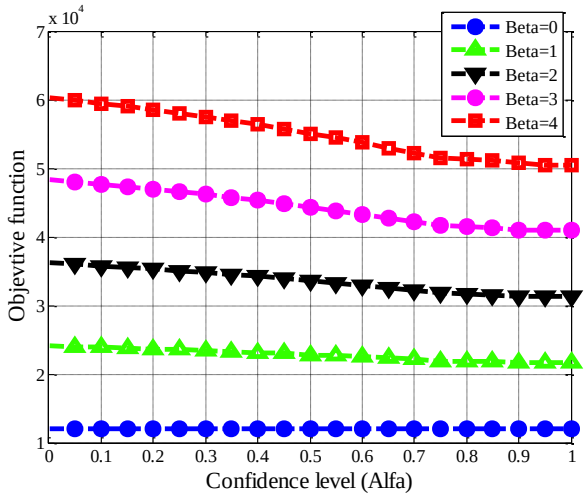

(a) β=0, ω=11

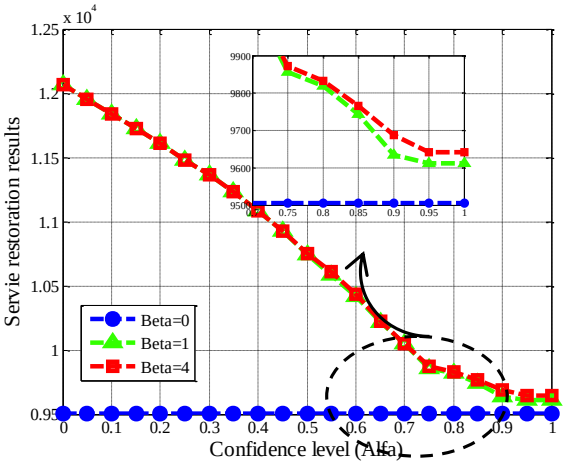

(b) β=0, ω=4

Fig. 14. (a) Objective function and (b) service restoration results for various confidence levels.

B) Case study 2

In this case, the condition of SR is considered that there isn't the ability of switching and reconfiguration in the network. By disconnecting the upstream network, the distributed energy sources along with the available electric vehicles in the parking lots start to restore the loads for a 4-hour period until the clearing the fault. The confidence level is assumed to be $\alpha = 0.9$. In this case, due to the increase in problem variables, the range of problem response to β changes has increased and another unique response has been obtained for $\beta = 4$. The results of this case are presented in Table 5 and Fig 10.

C) Case study 3

Because of the investment, installation, and maintenance costs of Remote controlled switches (RCSs), we are faced with the limitation of installing the RCSs in the network. In this paper, according to the network structure in Fig **??**.a, the location of the RCSs is considered to be lines 5, 16, 17, 18, and 19 from FLV1, FLV2, and FLV3. In this case, the ability of the reconfiguration in the network without the presence of electric vehicles is considered. Also, the confidence level is assumed to be α=0.9. This case is simulated and the results of SR values versus CVaR are shown in Table 6. The trend of changes in the objective function for the change in β is also shown in Fig 11.

D) Case study 4

Finally, in this case, both the ability to reconfiguration and the presence of electric vehicles are considered. The confidence level is assumed to be $\alpha = 0.9$. This case is simulated and the results of SR values and CVaR for changes from 0 to 4 in β are shown in Table 7. The trend of changes in the objective function for the change in β is also shown in Fig 12.

For more access to the details of the load restoration scheduling scheme, Fig 13 is prepared for the worst scenario ($\omega = 4$) and the best scenario ($\omega = 11$) in such a way that in three tiers, the optimal amount of the load that should be restored in each bus and related to each type is specified in 4 hours. As mentioned previously, it is assumed that loads E, Q, and G are equal in four-time steps with light colors in Fig 13, and three color shaded areas display different MGs with the three type distributed generators.

According to results of $\beta = 0$ in Table 7, load buses 1, 2, 3, and 4 are in the same restoration zone (MG1) and supported by DG1 and electric vehicles in stages 1, and 3. In the first stage, DG1 can only provide 80 kW to the bus and the rest of the power is supplied by the electrical and chemical energy stored in the electric vehicle. Also, load buses 5, 6, 7, 8, and 9, and load buses 10, 11, 12, and 13 are in the MG2 and MG3 restoration zones, respectively. In the second and fourth stages, load buses 1, 2, 3, 4, 13 supported by the resources of MG1, and load buses 5, 6, 7, 8, and 9, and load buses 10, 11, and 12 supported by the resources of MG1 and MG2, respectively. Then by reconnecting to the upstream network, the structure returns to its primary structure.

According to the results of the optimization algorithm for $\beta = 4$, the network structure remains constant for 4 hours until the clearing of the fault.

The confidence level is an important factor in determining the expected value of the objective function and CVaR. For this reason, different decision-makers may choose different values for this parameter depending on the conditions and the different risk priorities. To analyze the effect of the confidence level, the simulation results for comparison and analysis for different confidence levels are shown in Fig 14.

According to Fig 14(a) and 14(b), the objective function and SR remain constant in $\beta = 0$ which is related to risk-neutral situations. According to the mathematical model, it is clear that in the risk-neutral mode, the answer will be independent from the risk management, so the fluctuation in the value of confidence level will not affect the answer to the problem. However, the value of the objective function decreases in the risk-averse condition as the confidence level increases. As shown in Fig 14(a), the rate of change in the objective function increases with β, and it is 0%, 11.62%, 15.86%, 18.05%, and 19.4% for β from 0 to 4, respectively. It shows a direct relationship between the β and the effect of the confidence level on changes in the objective function. Also, the service restoration results in the risk-averse condition have a descending trend by increasing the confidence level according to Fig 14(b).

4. CONCLUSIONS

In this paper, a model is proposed to consider the risk management tool by uncertain parameters in the SR problem and self-healing mode. The objective is to maximize the restored loads and minimize the risk of the results. In five case studies, the impacts of risk weight, confidence level, and the presence of EVs & PHEVs in different conditions are investigated in order to control the effect of risk in the SR problem. These analyses have verified the performance of the proposed model and proved the importance of the risk control issue when formulating stochastic programming models. Analyzing the results shows that the risk assessment affects both the restoration schedule and switching in MGs. Meanwhile, according to the results, the robustness of the CVaR in compare to expected SR in all case studies have been increased. On the other hand, the value of CVaR in the

risk-neutral SR problem is less than that in the risk-constrained SR problem in all cases. This indicates a more risk-taking response by increasing β. For further studies, the development of the model and the addition of details related to the operation, as well as the production of scenarios, can be a field of study for further research.

REFERENCES

[1] Y. Wang, T. Huang, X. Li, J. Tang, Z. Wu, Y. Mo, L. Xue, Y Zhoe, T. Niu, S. Sun, "A Resilience Assessment Framework for Distribution Systems Under Typhoon Disasters," IEEE Access, Vol. 9, Nov 2021.

[2] W. Li, Y. Deng, M. Zhang, J. Li, Sh. Chen, S. Zhang, "Integrated Multistage Self-Healing in Smart Distribution Grids Using Decentralized Multiagent," IEEE Access, Vol. 9, Nov 2021.

[3] S.M Mohammadi-Hosseininejad, A. Fereidunian, A. Shahsavari, H. Lesani, "A Healer Reinforcement Approach to Self-Healing in Smart Grid by PHEVs Parking Lot Allocation," IEEE Trans. Ind. Inf., vol. 12, Dec 2016.

[4] J. R. Aguero, "Applying self-healing schemes to modern power distribution systems," in Proc. IEEE Power Energy Soc. Gen. Meeting, San Diego, CA, USA, pp. 1–4. 2012.

[5] E. Shahryari, H. Shayeghi, B. Mohammadi-Ivatloo, M. Moradzadeh, "Optimal energy management of microgrid in day-ahead and intra-day markets using a copula-based uncertainty modeling method.," J. Oper. Autom. Power Eng., vol. 2, pp. 86-96, 2019.

[6] H. Shayeghi, M. Alilou, "Multi-Objective Demand Side Management to Improve Economic and Environmental Issues of a Smart Microgrid," J. Oper. Autom. Power Eng., Vol. 9, No. 3, pp. 182-192, Dec. 2021.

[7] National Energy Technology Laboratory, "A systems view of the modern grid," 2007 [Online]. Available: https://www.netl.doe.gov/ , Accessed: 2018.

[8] N. AfsariArdabili, S.J. Seyedshenava, H. shayeghi, "Self-Healing Policy in Distribution Network Considering Technical Indices," Smart Grid Conf. (SGC), 2019.

[9] Y. Hsu, and H. Huang, "Distribution system service restoration using the artificial neural network approach and pattern recognition method," IEEE Proc. Gener. Transmiss. Distrib, vol. 142, no. 3, pp. 251–256, May 1995.

[10] Y. Fukuyama, and H. Endo, "A hybrid system for service restoration using expert system and genetic algorithm," in Proc. IEEE Int. Conf. Intell. Syst. Appl. Power Syst., Orlando, FL, USA, 1996, pp. 394–398.

[11] H. Farzin, M. Fotuhi-Firuzabad, and M. Moeini-Aghtaie, "Enhancing power system resilience through hierarchical outage management in multi-microgrids," IEEE Trans. Smart Grid, vol. 7, no. 6, pp. 2869-2879, Nov. 2016.

[12] E. Shahryari, H. Shayeghi, B. Mohammadi-ivatloo, M. Moradzadeh, "A copula-based method to consider uncertainties for multi-objective energy management of microgrid in presence of demand response," Energy, Vol. 175, pp. 879-890, 2019.

[13] Zh. Bie, P. Zhang, G. Li, B. Hua, M. Meehan, Xi. Wang, "Reliability Evaluation of Active Distribution Systems Including Microgrids," IEEE Trans. Power Syst., Vol. 12, 2012.

[14] Y. Xiang, J. Liu, Y. Liu, "Robust Energy Management of Microgrid With Uncertain Renewable Generation and Load," IEEE Trans. Smart Grid, Vol. 7, 2016.

[15] A. Hussain, A. Rousis, I. Konstantelos, G. Strbac, J. Jeon, H. Kim, "Impact of Uncertainties on Resilient Operation of Microgrids: A Data-Driven Approach," IEEE Access, Vol. 7, 2019.

[16] J. Liu, H. Chen, W. Zhang, B. Yurkovich, G. Rizzoni, "Energy Management Problems Under Uncertainties for Grid-Connected Microgrids: a Chance Constrained Programming Approach," IEEE Trans. Smart Grid, Vol. 8, 2017.

[17] N. Vesperman, T. Hamacher, J. Kazempour "Risk Trading in Energy Communities," IEEE Trans. Smart Grid, Vol. 12, 2021.

[18] R. Mieth, M. Roveto, Y. Dvorkin, "Risk Trading in a Chance-Constrained Stochastic Electricity Market," IEEE Control Syst. Lett., Vol. 5, 2021.

[19] M. Bao, Y. Ding, X. Zhou, C. Guo, C. Shao, "Risk assessment and management of electricity markets: A review with suggestions," CSEE J. Power Energy Syst., Vol. 7, 2021.

[20] M. Negnevitsky, D. Nguyen, M. Piekutowski, "Risk Assessment for Power System Operation Planning With High Wind Power Penetration," EEE Trans. Power Syst., Vol. 30, 2015.

[21] L. Costa, F. Thome, J. Garcia, M. Pereira, "Reliability-Constrained Power System Expansion Planning: A Stochastic Risk-Averse Optimization Approach," IEEE Trans. Power Syst., Vol. 36, 2021.

[22] M. Izadi, A. Safdarian, "Financial Risk Evaluation of RCS Deployment in Distribution Systems," IEEE Syst. J., Vol. 13, 2019.

[23] A. Dolatabadi, B. Mohammadi-Ivatloo, "Stochastic Risk-Constrained Optimal Sizing for Hybrid Power System of Merchant Marine Vessels," IEEE Trans. Ind. Inf., Vol. 14, 2018.

[24] A. Conejo, L, Baringo, S.J Kazempour, A. Siddiqui, "Investment in Electricity Generation and Transmission Decision Making under Uncertainty," springer, 2016.

[25] A. Conejo, M. Carrion, J. Morales, "Decision Making Under Uncertainty in Electricity Markets," Springer, New York, 2010.

[26] S. Civanlar, J. J. Grainger, H. Yin and S. S. H. Lee, "Distribution feeder reconfiguration for loss reduction" IEEE Trans. Power Deliv., vol. 3, no.3, pp. 1217–1223, 1988.

[27] Z. Liu, D. Wang, H. Jia, N. Djilali, W. Zhang, "Aggregation and bidirectional charging power control of plug-in hybrid electric vehicles: generation system adequacy Analysis," IEEE Trans. Sustain. Energy,Vol. 6, pp. 325–35, 2015.

[28] C. Guille and G. Gross, "The integration of PHEV aggregations into a power system with wind resources," in Proc. Bulk Power Syst. Dyn. Control Symp., Buzios, Brazil, pp. 1–9, Aug. 2010.

[29] H. Momen, A. Abessi, Sh. Jadid, M. Shafie-khah, J. Catalao, "Load restoration and energy management of a microgrid with distributed energy resources and electric vehicles participation under a two-stage stochastic framework," Int. J. Electr. Power Energy Syst., Vol. 133, Dec 2021.

[30] M.R. Bussieck, A. Pruessner, "Mixed-integer nonlinear programming," SIAG/OPT Newsl. Views News, Vol. 14, pp. 19–22, 2003.

[31] H. Shin, R. Baldick, "Plug-in electric vehicle to home (V2H) operation under a grid Outage," IEEE Trans. Smart Grid, Vol. 8(4), pp.2032–41, 2017.

[32] J.R. Birge and F. Louveaux. "Introduction to stochastic programming," Springer- Verlag, New York, 1997.

[33] M. Zadsar, M.R Haghifam, S.M Miri, "Approach for self-healing resilient operation of active distribution network with microgrid," IET Gener. Transm. Distrib., Vol. 11, Iss. 18, pp. 4633-4643, 2017.

[34] B. Zhao, X. Dong, J. Bornemann, "Service Restoration for a Renewable-Powered Microgrid in Unscheduled Island Mode," IEEE Trans. Smart Grid, Vol. 6, no. 3, MAY 2015.